

# **Supporting Information:**

## **NMRlipids IV: Headgroup & glycerol backbone structures, and cation binding in bilayers with PS lipids**

Pavel Buslaev,<sup>†</sup> Tiago M. Ferreira,<sup>‡</sup> Ivan Gushchin,<sup>†</sup> Matti Javanainen,<sup>¶</sup> Batuhan Kav,<sup>§</sup> Jesper J. Madsen,<sup>||</sup> Markus Miettinen,<sup>§</sup> Josef Melcr,<sup>¶</sup> Ricky Nencini,<sup>¶</sup> O. H. Samuli Ollila,<sup>\*,¶</sup> and Thomas Piggot **Authorlist is not yet complete<sup>#</sup>**

<sup>†</sup>*Moscow Institute of Physics and Technology*

<sup>‡</sup>*Halle, Germany*

<sup>¶</sup>*Institute of Organic Chemistry and Biochemistry, Academy of Sciences of the Czech Republic, Prague 6, Czech Republic*

<sup>§</sup>*Potsdam, Germany*

<sup>||</sup>*Department of Chemistry, The University of Chicago, Chicago, Illinois 60637, United States of America*

<sup>⊥</sup>*Institute of Biotechnology, University of Helsinki*

<sup>#</sup>*Southampton, United Kingdom*

E-mail: samuli.ollila@helsinki.fi

## S1 Simulated systems

### S1.1 CHARMM36

*POPC bilayer.* Previously published values<sup>1</sup> calculated from the data available from Ref. 2 are used.

*DOPS and POPS bilayers.*

The data in Table I and Refs 3–5 [T. Piggot, please write simulation details](#)

*POPC:POPS mixtures without additional ions*

Simulations of POPC:POPS (5:1) mixture containing total 132 (110:22) lipids with potassium and sodium counterions were ran using CHARMM36 force field. The data are available from Refs. 6 and 7, respectively[T. Piggot, please write simulation details](#).

Simulations of POPC:POPS (5:1) ans POPC:POPS (1:1) mixtures containing total 300 lipids with potassium counterions were ran using CHARMM36 force field. The data are available from Refs. ? [J. Madsen, please write simulation details](#).

*POPC:POPS (5:1) mixtures with additional monovalent ions.* Systems containing total 132 (110:22) lipids were simulated with the additional potassium and sodium counterion concentrations of ~450 mM and 890 mM using CHARMM36 force field at 298 K. The data, force field and input files generated using parameters given by CHARMM-GUI<sup>8,9</sup> are available from Refs. 10–13.

*POPC:POPS (5:1) mixtures with additional calcium*

POPC:POPS (5:1) mixtures containing total 300 (250:50) lipids were simulated with the additional calcium concentrations [J. Madsen, please write simulation details](#).

## S1.2 CHARMM36ua

*DOPS and POPS bilayers.*

The data in Table I and Refs 14,15 T. Piggot, please write simulation details

## S1.3 MacRog

*POPC bilayers.* Simulation data available from Ref. 16. For example this data set has pretty good description of simulation details in the reference. I am not sure how much we should repeat these in here.

The POPC bilayer consisting of a total of 128 lipids was constructed from single lipid structure taken from Ref.<sup>?</sup> The bilayer was hydrated by a total of 5120 water molecules, corresponding to 40 water molecules per lipid.

The MacRog lipid parameters,<sup>?</sup> obtained from,<sup>?</sup> were used, along with the TIP3P water model.<sup>?</sup> The simulation parameters were identical to those used for POPC/POPC mixtures with the MacRog force field, see below. The simulation was run for 200 ns, out of which ?? ns: (this is not tabulated in the MS or the SI) were used for analyses.

*POPS bilayers.*

The data in Table I and Refs 17,18 T. Piggot and M. Javanainen, please write simulation details

Piggot: please write about system with Na<sup>+</sup> counterions.

This membrane was further simulated after replacing Na<sup>+</sup> counterions by K<sup>+</sup> ones, which were described by the Åqvist parameters.<sup>?</sup> Other topologies were unchanged. The simulation parameters were the same as used for the POPC/POPS mixtures with the MacRog force field, see below. The simulation was run for 200 ns, out of which 150 ns was used in the analyses.

*POPC:POPS (5:1) mixtures with additional potassium ions*

The data in Table II and Refs 19,20

The bilayers containing a total of 120 POPC and 24 POPS molecules distributed evenly among the two leaflets were set up using CHARMM-GUI.<sup>8,9</sup> The bilayers were solvated by 5760 water molecules, corresponding to 40 water molecules for lipid. Additionally, 24 potassium ions were added to neutralize the charge of the POPS head groups.

These bilayers were simulated in the presence of counterions only, as well as together with different concentrations of CaCl<sub>2</sub> or KCl. For the former, concentrations of 100 mM, 300 mM, 1 M, and 3 M were considered, which corresponded to the amounts of 10/20, 31/62, 104/208, and 311/622 of Ca<sup>2+</sup>/Cl<sup>-</sup> ions. For membranes with KCl, concentrations of 500 mM, 1 M, 2 M, and 3 M were considered, corresponding to 52, 104, 208, or 311 pairs of K<sup>+</sup> and Cl<sup>-</sup> ions.

The lipids were described using the MacRog model.<sup>???</sup> The POPC topologies were obtained from Ref. ?, whereas the POPS topology was adapted from Ref. ?. Notably, the chains were reversed in order to modify OPPS into POPS. Unlike the D stereoisomer present in Ref.,<sup>?</sup> the POPS head group conformations generated by CHARMM-GUI are in the naturally occurring L stereoisomer. TIP3P model<sup>?</sup> was used for water, and the Åqvist parameters,<sup>?</sup> standard for the OPLS force field, were employed for the ions.

The simulation parameters were taken from Ref. ?. Periodic boundary conditions were employed in all dimensions. The list of neighbors was updated every step I used nstlist=1 because it's used in the mdp in the article quoted. In DOI: 10.1021/jp5016627, nstlist=10 is used The Lennard-Jones interactions were cut off at 1 nm, whereas the smooth particle mesh Ewald algorithm<sup>?</sup> was used for electrostatics. Dispersion correction<sup>?</sup> was applied to both energy and pressure. Temperature was kept constant at 298 K using the Nosé–Hoover thermostat.<sup>??</sup> The lipids and the solvent were coupled separately, and a time constant of 0.4 ps was employed. Pressure was maintained semi-isotropically at 1 bar using the Parrinello–Rahman barostat with a time constant of 1 ps.<sup>?</sup> All non-water bonds were constrained with the LINCS algorithm,<sup>??</sup> whereas the bonds in water molecules were constrained using SETTLE.<sup>?</sup> The integration time step was set to 2 fs, and the simulations were performed

either for 400 ns (only counterions), 300 ns (systems with KCl), or 600 ns (systems with CaCl<sub>2</sub>). The last 250, 200, or 300 ns of the simulations were included in the analyses, respectively.

## S1.4 Lipid17

*DOPS and POPS bilayers.*

The data in Table I and Refs 21–24 B. Kav and M. Miettinen, please write simulation details

*POPC:POPS (5:1) mixtures with additional potassium and sodium ions*

The data in Table II and Refs 25–28 B. Kav and M. Miettinen, please write simulation details

*POPC:POPS (5:1) mixtures with additional calcium*

The data in Table II and Refs 29 J. Melcr, please write simulation details

## S1.5 Berger

*POPC bilayers.* Previously published simulation<sup>30</sup> available from Ref. 31 was used for POPC at 310 K.

*DOPS and POPS bilayers.*

The data in Table I and Refs 32,33 T. Pigget, please write simulation details

*POPC:POPS (4:1) mixtures with additional sodium and calcium ions.* Previously published simulations with the additional amount of sodium<sup>34</sup> available from Ref. 35 and with the additional amounts of calcium<sup>36</sup> available from Refs. 37,38 were used. The additional sodium ions were removed from the structure file of the simulation with excess amount of sodium<sup>35</sup> to generate the initial structure for the reference simulation with sodium counterions only.

The data, input and force field parameter files of the reference simulation are available from

Ref. 39. The simulation details of this are not clearly described in Zenodo repository, but can be read from the mdp file available there. Should we write the detailes here or not?

## S1.6 GROMOS-CKP and GROMOS-CKPM

CKPM refers to the version with Berger/Chiu NH<sub>3</sub> charges compatible with Berger (i.e. the NH<sub>3</sub> group having the same charges as in the N(CH<sub>3</sub>)<sub>3</sub> group of the PC lipids; 'M' stands for Mukhopadhyay after the first published Berger-based PS simulation that used these charges<sup>40</sup>) and CKP refers to the version with more Gromos compatible version (i.e. the charges for the NH<sub>3</sub> group taken from the lysine side-chain). T. Piggot, please write the description of force field.

*DOPS and POPS bilayers.*

The data in Table I and Refs. 41–44 T. Piggot, please write simulation details

*POPC:POPS (5:1) mixtures without additional ions*

The data in Table II and Refs. 45,46 T. Piggot, please write simulation details

## S1.7 Slipids

*DOPS and POPS bilayers.*

The data in Table I and Refs. 47–49. T. Piggot and F. Favela, please write simulation details

## S2 Electrometer concept in PC lipid bilayers mixed with negatively charged lipids

The electrometer concept is based on the empirical observations that the order parameters of  $\alpha$  and  $\beta$  carbons in PC lipid headgroup decrease (increase) proportionally to the bound positive (negative) charge<sup>50–53</sup> (Fig. S1). Therefore, the headgroup order parameters can be used to measure the ion binding affinity to lipid bilayers containing PC lipids.<sup>50–52,54–56</sup>

Changes of the headgroup order parameters of negatively charged PS and PG lipids are also systematic, but less well characterized.<sup>54–57</sup> Therefore, the ion binding affinity to negatively charged bilayers can be better characterized measuring the PC headgroup order parameters from mixed bilayers.<sup>54–58</sup>

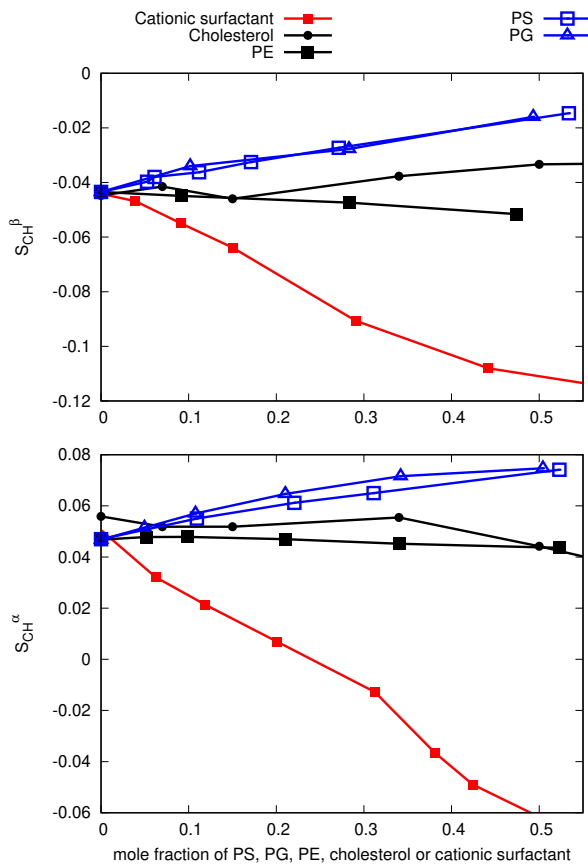


Figure S1: Headgroup order parameters of POPC measured from mixtures with PS (bovine brain), POPG, POPE, cholesterol and cationic dihexadecyldimethylammonium bromide (DHAB) surfactant.<sup>53,59,60</sup> Signs are taken from separate experiments.<sup>61,62</sup>

When using the PC headgroup order parameters to evaluate the ion binding affinity to a bilayer containing anionic lipids, it is important to note that the order parameters increase due to the addition of negative charged lipids according to the electrometer concept<sup>52,59</sup> (Fig. S1). Therefore, the PC headgroup order parameters are larger in mixtures with anionic lipids than in pure lipid bilayers. This is evident also in the headgroup order parameters of POPC in bilayers with different amounts anionic lipids without added calcium (Fig. S2). Upon addition of  $\text{CaCl}_2$ , the order parameters decrease and reach the values of pure PC bilayer close to the  $\text{CaCl}_2$  concentrations of  $\sim 50\text{-}300\text{mM}$ , depending on the amount of negatively charged lipids in the mixture (Fig. S2). Around these concentrations the positive charge of bound  $\text{Ca}^{2+}$  cancels the negative charge lipids, resulting to a neutral membrane. Above such concentrations, the specific binding of calcium leads to the overcharging of the membrane.

Because the POPC headgroup order parameters in mixtures with different amounts of anionic lipids but without additional salt are not equal, the binding affinity of calcium can be better compared by plotting the changes of order parameters as a function of added calcium. As expected, such a plot reveals more pronounced order parameter decrease in systems with larger fractions of negatively charged lipids (Fig. S3), indicating an increase in the calcium binding affinity with the increasing amount of negatively charged lipids in membranes. In conclusion, the presented empirical comparison of headgroup order parameter changes from various mixtures of POPC and anionic lipids with added calcium gives physically consistent results, suggesting that the electrometer concept can be used to determine the cation binding affinity also to the lipid bilayers containing mixtures of PC and anionic lipids.

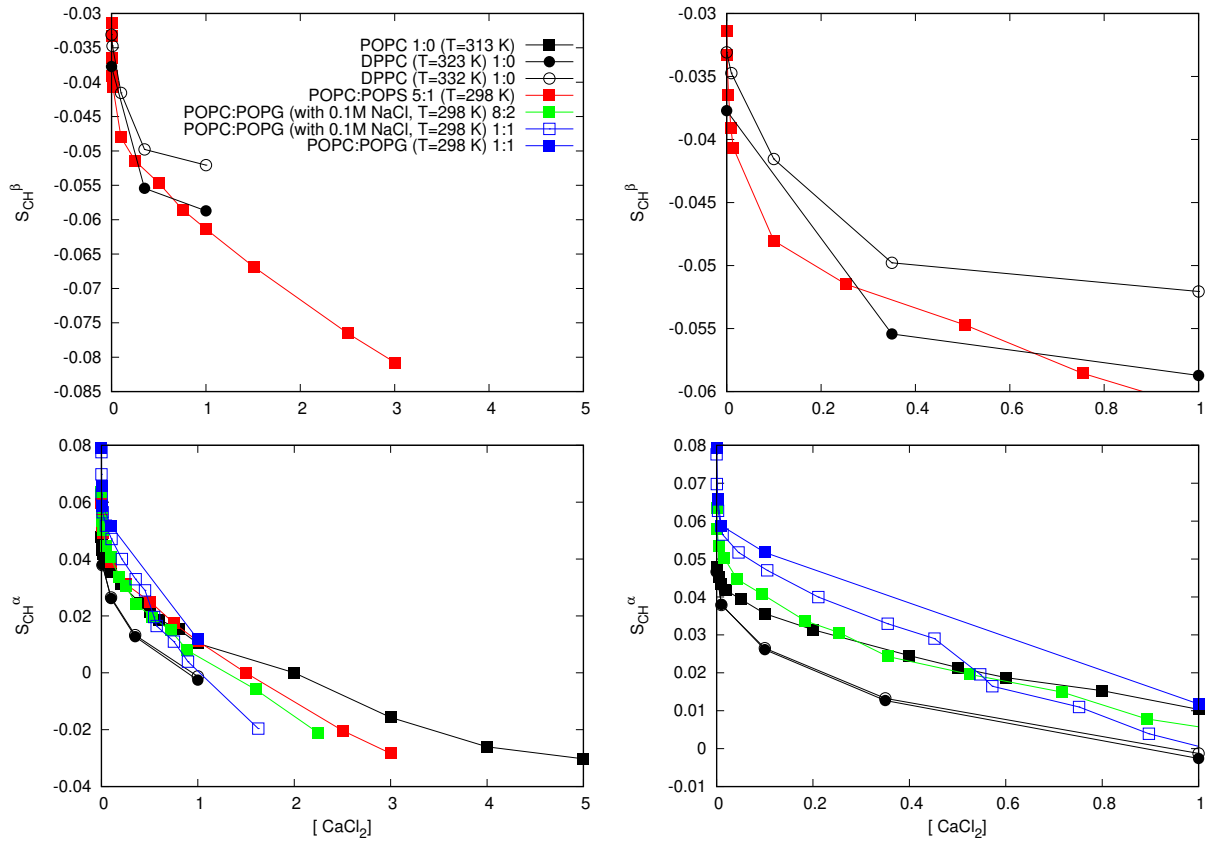


Figure S2: Headgroup order parameters of POPC as a function of  $\text{CaCl}_2$  concentration from experiments with different mole fractions of negatively charged lipids (left column). Right column shows the same data zoomed to the concentrations below 1M. Data for Pure DPPC from Ref. 50, for pure POPC from Ref. 51, for POPC:POPS (5:1) mixture from Ref. 56, for POPC:POPG (8:2,1:1) mixtures with 0.1M NaCl from Ref. 55 and for POPC:POPG (1:1) mixture data without NaCl from Ref. 54.

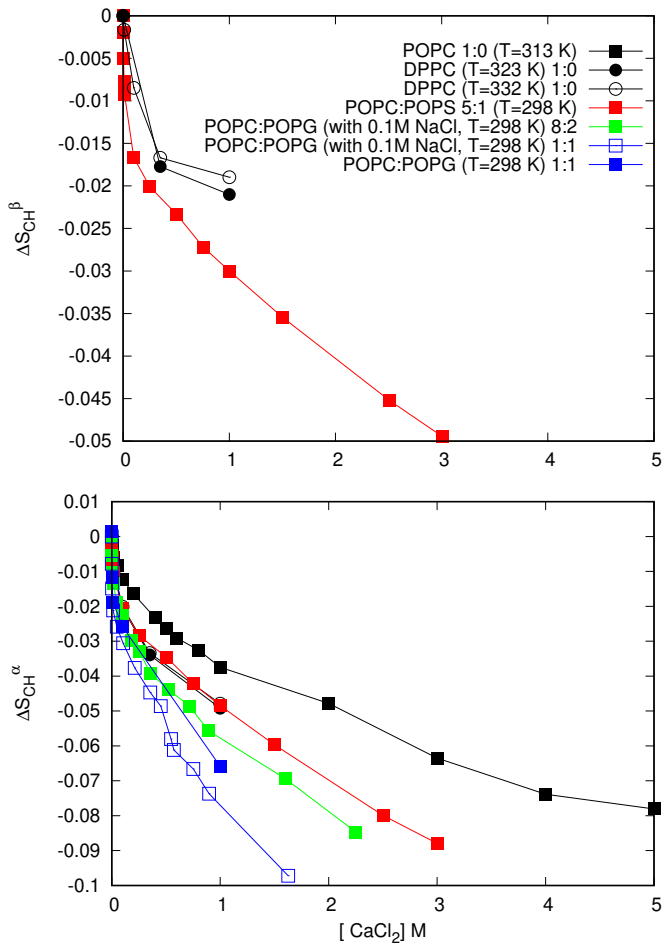


Figure S3: Changes of POPC headgroup order parameters as a function of  $\text{CaCl}_2$  measured from mixed bilayers containing different amounts of anionic lipids. The original data is the same as in figure S2.

### S3 Calibration of PC headgroup order parameter response to the bound cations

Before using the headgroup order parameters to compare ion binding affinity between simulations and experiments, the response of the order parameters to the bound charge in simulations should be quantified against experiments.<sup>63,64</sup> In our previous work,<sup>63</sup> the ratio  $\Delta S_{\text{CH}}^{\beta}/\Delta S_{\text{CH}}^{\alpha}$  was in good agreement with the experiments<sup>50</sup> in the Lipid14 model, but was underestimated by other models. In the more recent study,<sup>64</sup> the headgroup order parameter responses were compared more carefully with the experiments of cationic dihexadecyldimethylammonium bromide (DHAB) surfactants in POPC bilayer.<sup>53</sup> The comparison reveals that the both headgroup order parameters in the Lipid14 model are too sensitive to the bound charge, while CHARMM36 gives better agreement for the  $\alpha$  carbon (Fig. S4). Therefore, the headgroup order parameter response to the bound charge is actually more realistic in CHARMM36 model than in the Lipid14. In the latter, both order parameters are equally too sensitive to the bound cations giving a good result for the  $\Delta S_{\text{CH}}^{\beta}/\Delta S_{\text{CH}}^{\alpha}$  ratio. The ratio was overestimated for the CHARMM36 model because the  $\beta$ -carbon order parameter is relatively more sensitive than the  $\alpha$ -carbon order parameter. These results have to be taken into account when analysing the ion binding affinities using headgroup order parameters in simulations. However, we conclude that the discrepancies arising from the sensitivity of lipid headgroup to bound charge are typically smaller than the discrepancies arising from ion binding affinity.

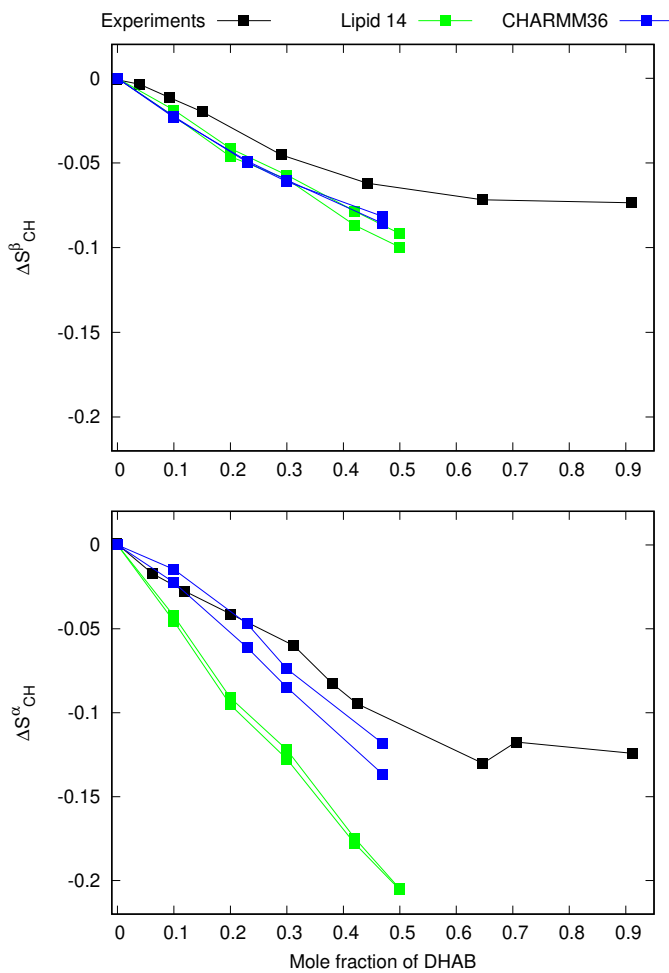


Figure S4: Responses of headgroup order parameters to the fixed amount of cationic surfactants in POPC bilayer from simulations and experiments.<sup>53</sup> The simulation results for Lipid14 are directly from Ref. 64. The CHARMM36 simulation data and details are available from Ref. 65.

## S4 Effect of the definition of concentration on the headgroup order parameters as a function of ion concentration.

Previous studies using the electrometer concept to assess the ion binding affinity to lipid bilayers report ion concentrations either in water before solvating the lipids (buffer concentration)<sup>50,56,63</sup> or in bulk water after solvating the lipids (bulk concentration).<sup>51,64</sup> In this work, we use the former definition to be consistent with the reference experimental data.<sup>56</sup> The difference between these two concentrations increases with the increasing ion binding affinity. However, the difference is essentially negligible in the recent model<sup>64</sup> with realistic ion binding affinity (Fig. S5).

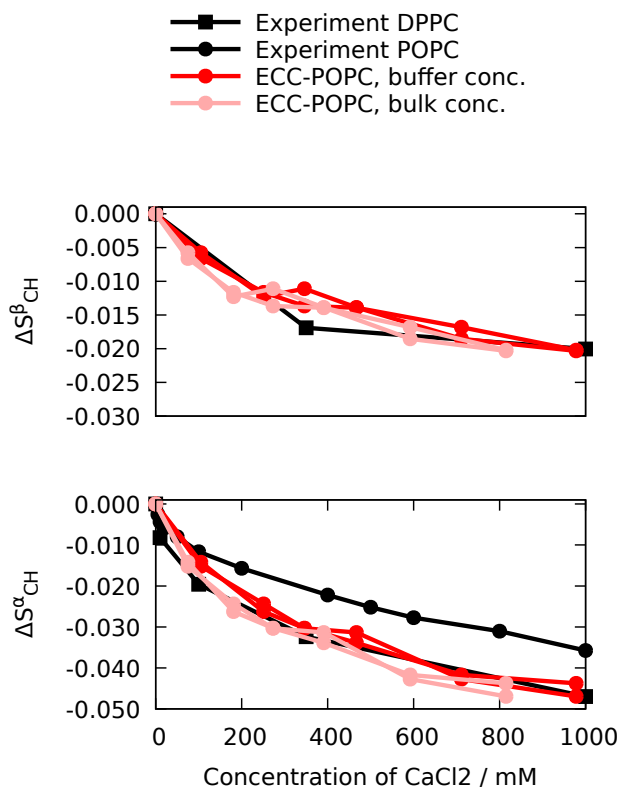


Figure S5: Changes of the headgroup order parameters as a function of  $\text{CaCl}_2$  concentration using two possible definitions of ion concentration from the recent force field with realistic calcium binding affinity to a POPC bilayer<sup>64</sup> together with the experimental data.<sup>50,51</sup>

## S5 Dipolar slices of the R-PDFL experiment

Slices of the R-PDFL spectra (Fig. S6) show a single splitting for the  $\beta$ -carbon with the order parameter value of 0.11, and a superposition of a large and a very small splitting for the  $\alpha$ -carbon. The larger splitting from the  $\alpha$ -carbon gives a order parameter value of 0.09, while the numerical value from the small splitting cannot resolved with the available resolution.

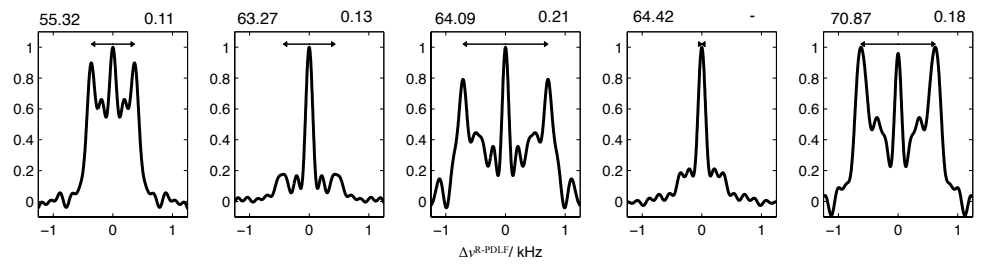


Figure S6: Dipolar coupling slices from the R-PDFL experiment.  
Labeling of carbons and explanations of numbers (chemical shift and order parameter) would be good. The splitting corresponding the larger  $\alpha$ -carbon order parameter should be also shown. Also, the size of the figure in the file may not be optimal.

## **S6 Dihedral angle distributions of the headgroup and glycerol backbone regions of PS lipids from different simulation models**

The dihedral angles and structures of the glycerol backbone and headgroup regions of POPS lipids show wide variety between different simulation models (Figs. S7, S8 and S9). Detailed discussion of the structural differences is limited by the lack of realistic model that would correctly reproduce the headgroup and glycerol backbone order parameters. However, some structural characteristics of PS headgroup can be suggested based on the best available models (Figs. S10, S11 and S12), as discussed in the main text. The glycerol backbone structures are not discussed in this work because our focus is on PS headgroup. However, the data presented here can be useful for future investigations.

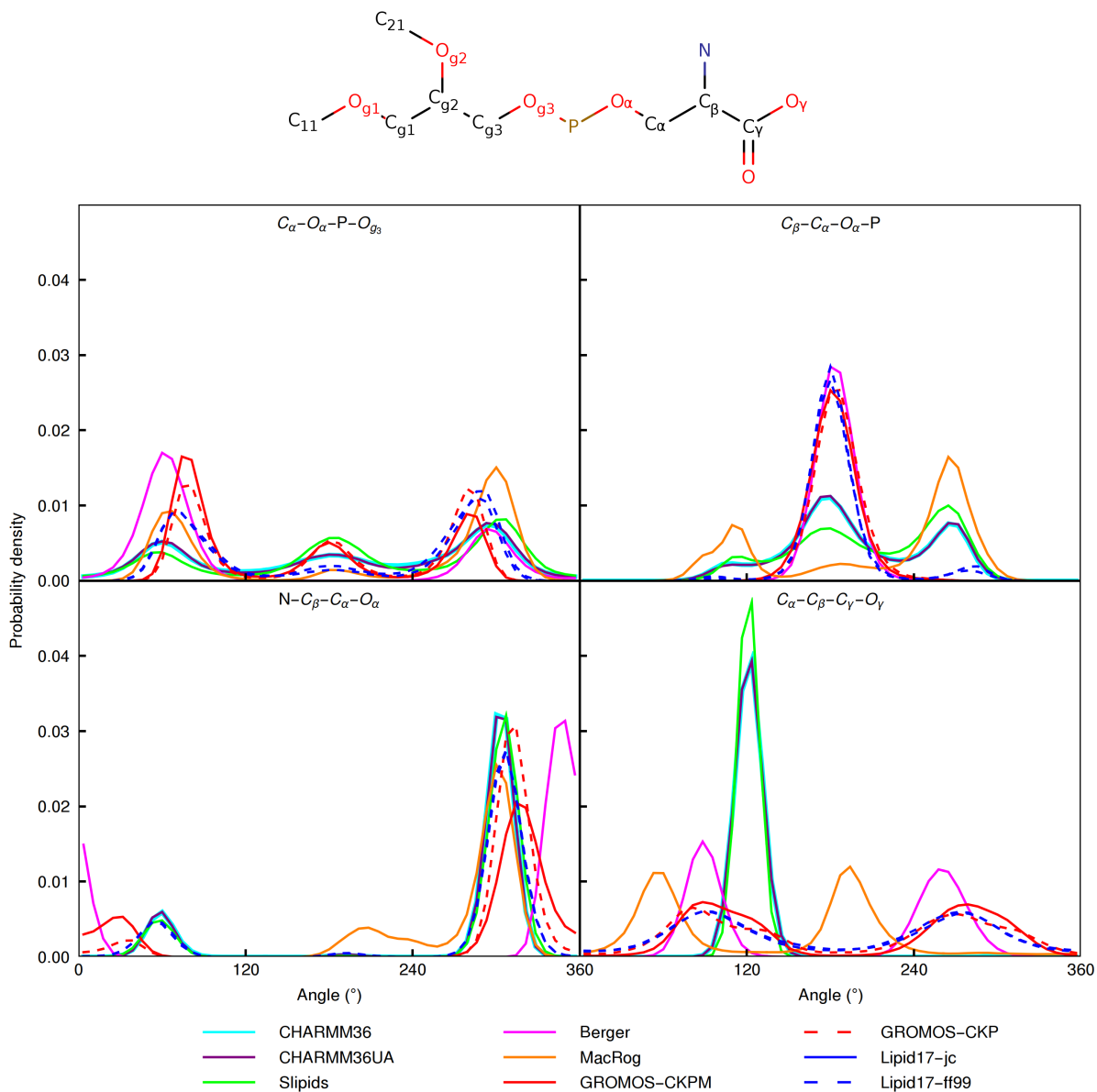


Figure S7: Dihedral angle distributions of the headgroup region of POPS from different simulation models.

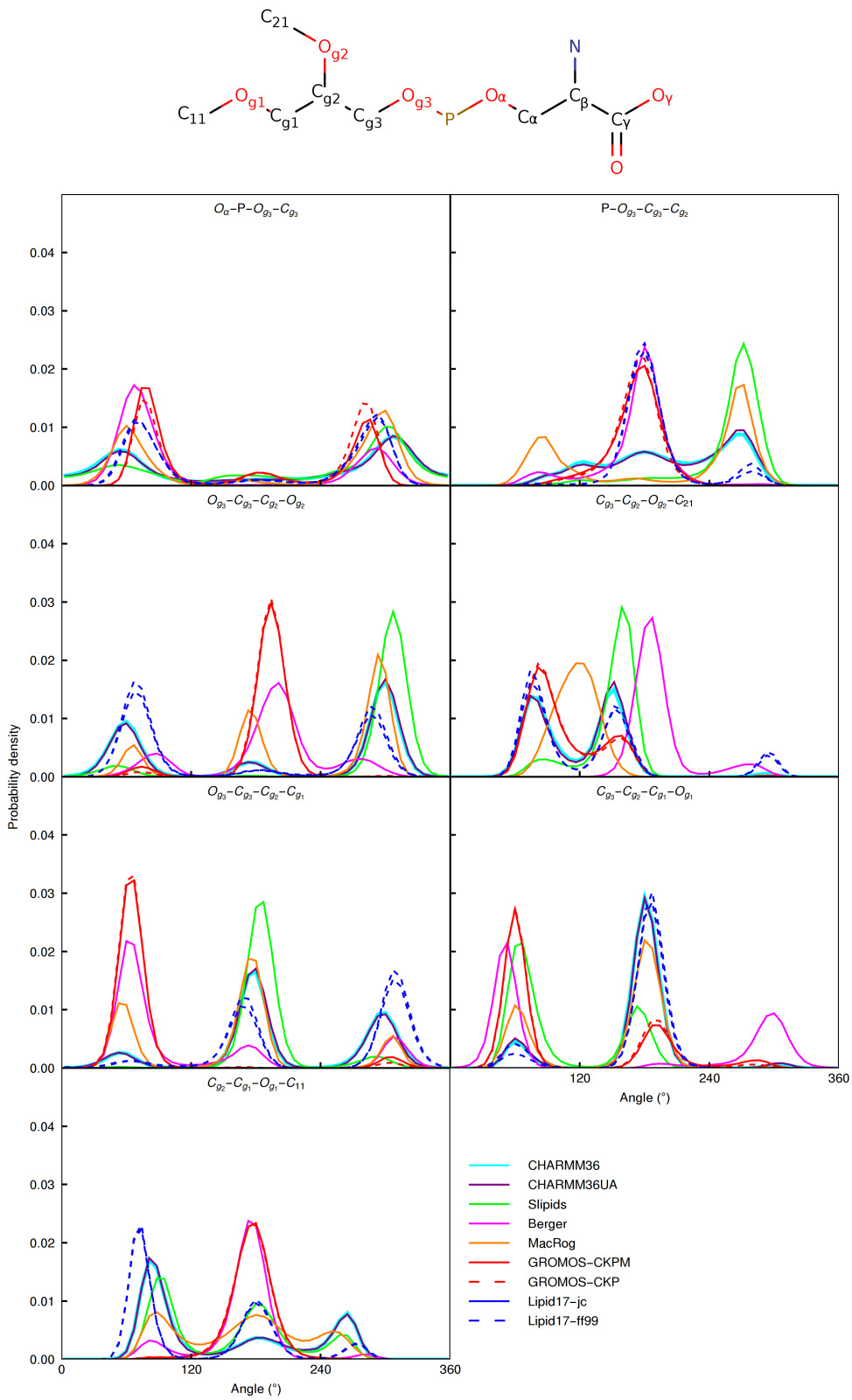


Figure S8: Dihedral angle distributions of the glycerol backbone region of POPS lipids from different simulation models.

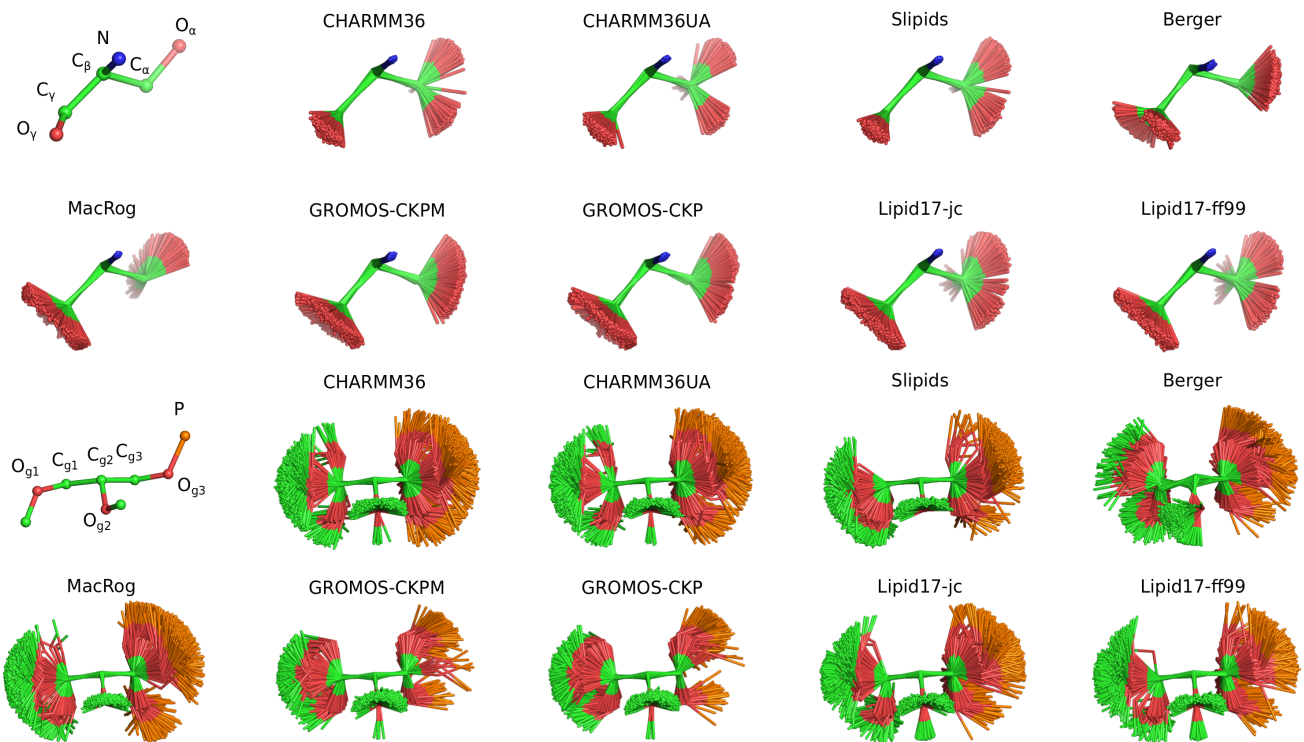


Figure S9: Overlayed snapshots of the glycerol backbone and headgroup regions from different POPS simulations.

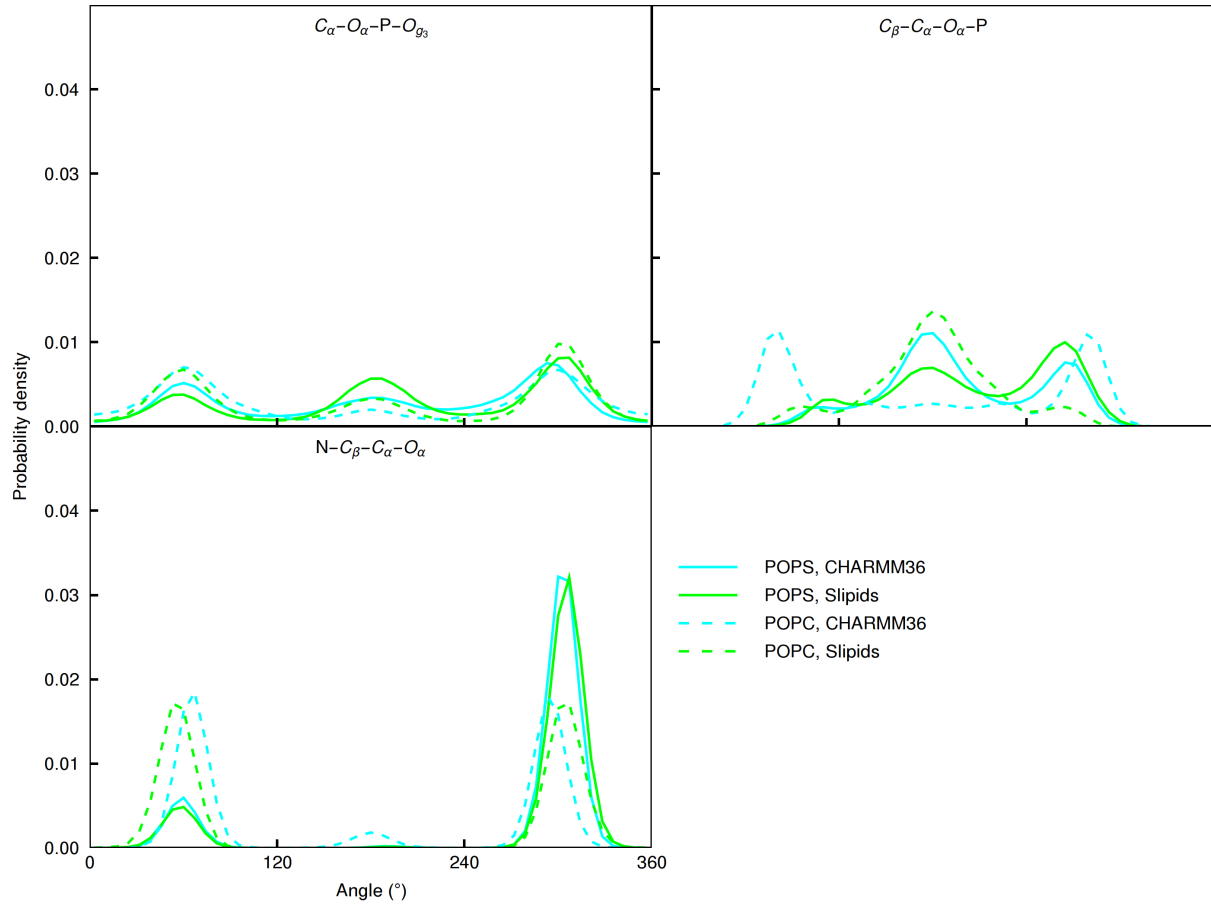


Figure S10: Dihedral angle distributions of the headgroup regions from CHARMM36 and Slipids simulations compared between the POPC and POPS lipids. The CHARMM36 POPC simulation is from Ref. 66 and Slipids POPC from Ref. 67.

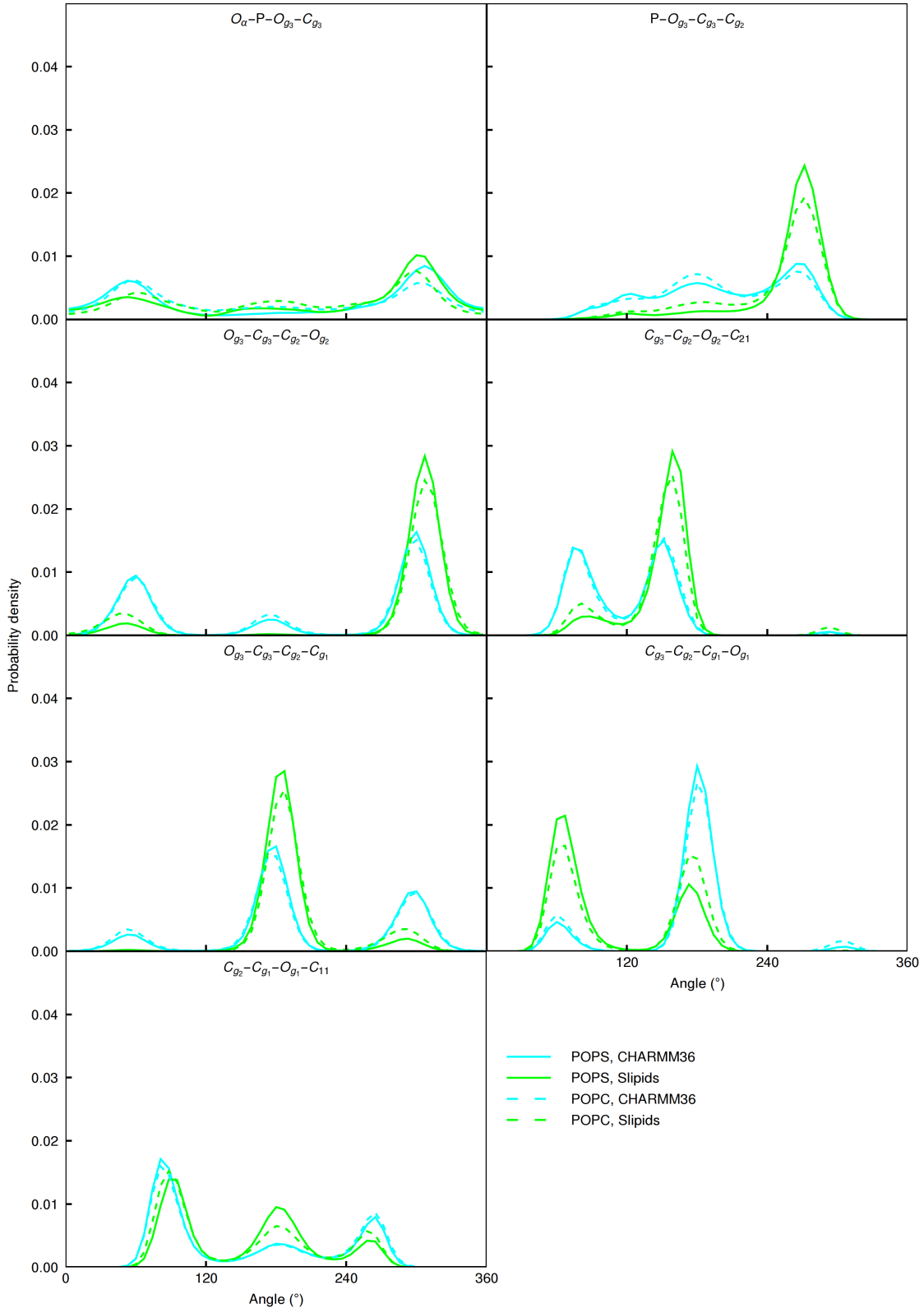


Figure S11: Dihedral angle distributions of the glycerol backbone regions from CHARMM36 and Slipids simulations compared between the POPC and POPS lipids. The CHARMM36 POPC simulation is from Ref. 66 and Slipids POPC from Ref. 67.

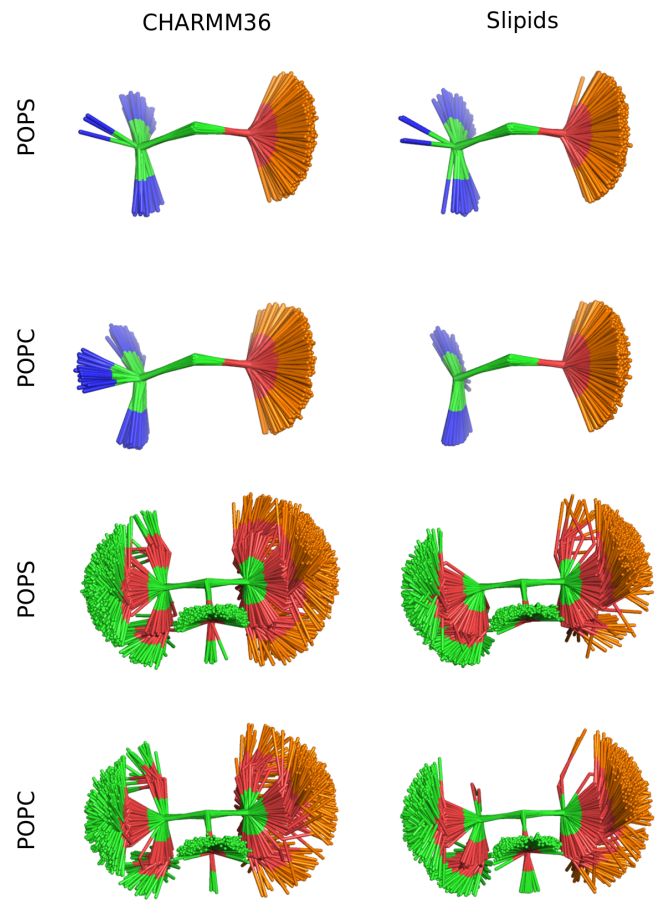


Figure S12: Overlayed snapshots of the headgroup and glycerol backbone regions from CHARMM36 and Slipids simulations compared between the POPC and POPS lipids. The CHARMM36 POPC simulation is from Ref. 66 and Slipids POPC from Ref. 67.

## S7 Headgroup response to the additional counterions in POPC:POPS (5:1) mixtures

To evaluate counterion binding in different simulation models against experimental data,<sup>56</sup> we plot the headgroup order parameters measured from POPC:POPS 5:1 mixture as a function of different monovalent ions added to the buffer (Fig. S13). Experimental order parameters of POPC headgroup in the mixture are available as a function of LiCl and KCl concentrations, while POPS headgroup order parameters are measured also as a function of NaCl. Lithium interacts more strongly with PS headgroups than other monovalent ions,<sup>56,57,68–70</sup> as also observed for PC headgroups.<sup>71</sup> The different binding behaviour is evident also in the changes of PS headgroup order parameters, which decrease with the addition of lithium but increase with the addition of sodium or potassium (Fig. S13). POPC headgroup order parameters exhibit a clear decrease as a function of LiCl concentration but only modest changes as a function of KCl concentration, indicating significant Li<sup>+</sup> binding but only weak K<sup>+</sup> binding to the mixture when interpreted using the electrometer concept.<sup>50–52</sup>

In simulations with Berger and CHARMM36 models, the responses of headgroup order parameter of both POPC and POPS to the added sodium or potassium are more similar to the experiments with LiCl (Fig. S13), indicating overestimated binding affinity of sodium and potassium in these simulations. The MacRog simulations with potassium exhibit weaker counterion binding affinity (Fig. S14), but significantly larger error bars and less systematic changes in the order parameters (Fig. S13). Similar unsystematic behaviour was also observed in the simulations of Lipid14/17 model with the additional counterions,<sup>25–28</sup> for which the data is not shown due to the formation of ion clusters in water with relatively low (1 M) ion concentrations (Fig. S15). Appearance of such clusters also in the MagRog simulations with 4 M concentration of KCl could explain the unsystematic changes of the order parameters in this model with the added KCl. In conclusion, the results are in line with the section 24 in the main text, suggesting that the MacRog simulations with KCl give the most realistic

surface charge at the lipid bilayer interface among the tested simulation models.

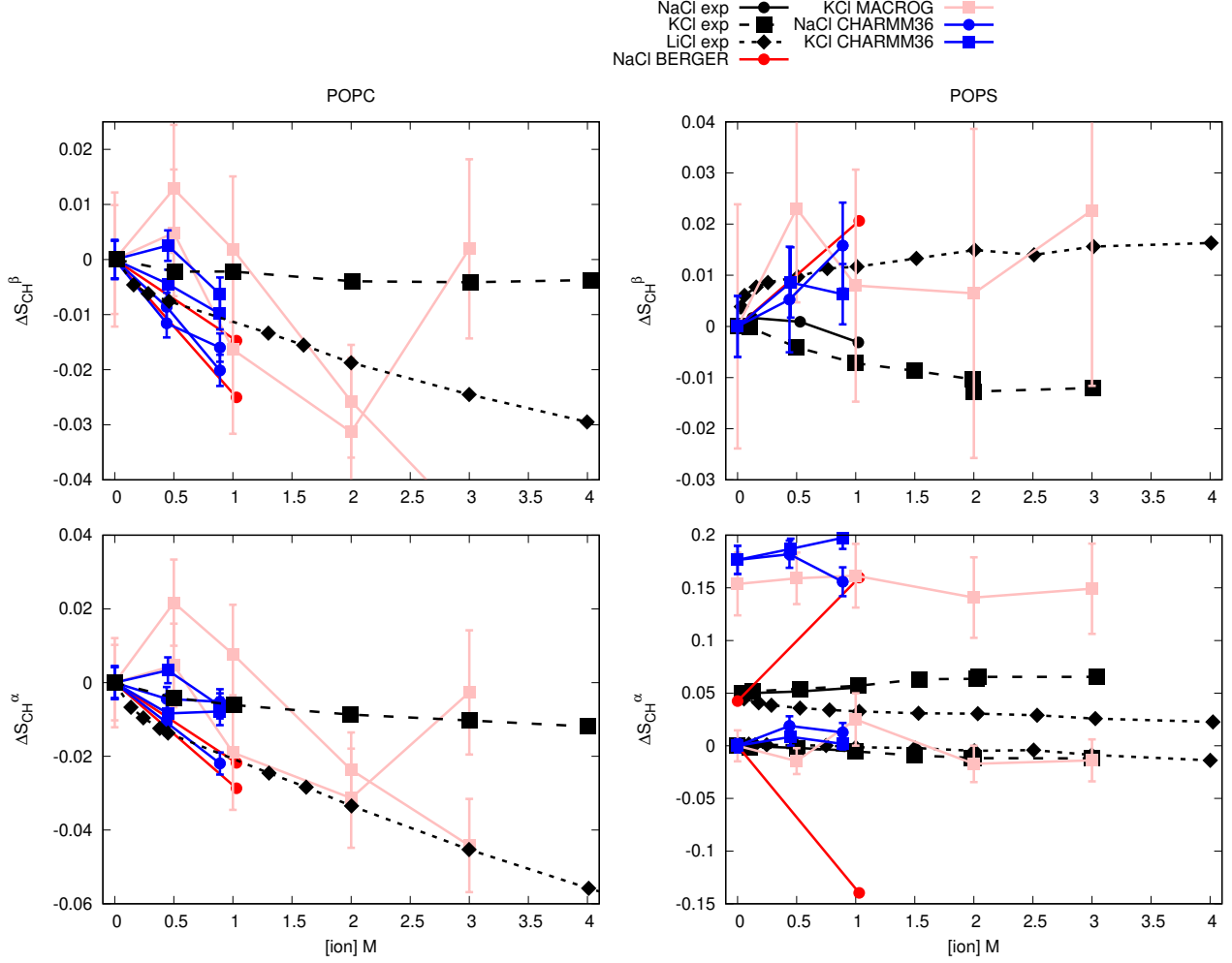


Figure S13: Changes of the PC (left) and PS (right) headgroup order parameters as a function of added NaCl, KCl and LiCl from POPC:POPS (5:1) mixture at 298 K (except Berger simulations are (4:1) mixture at 310 K). The experimental data is from Ref. 56. The values from counterion-only systems are set as a zero point of y-axis. To correctly illustrate the significant forking of the  $\alpha$ -carbon order parameter in PS headgroup (bottom, right), the y-axis is transferred with the same value for both order parameters such that the lower order parameter value is at zero.

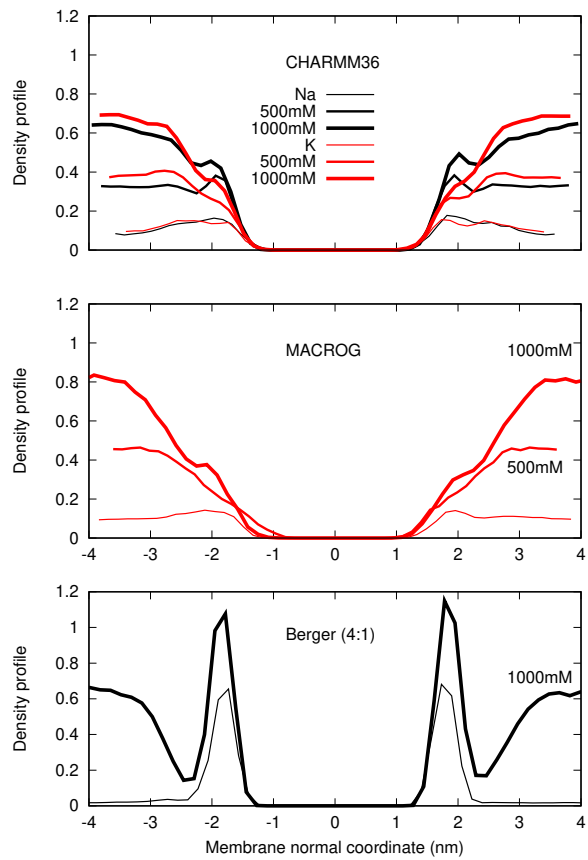


Figure S14: Counterion density distributions from PC:PS mixtures.

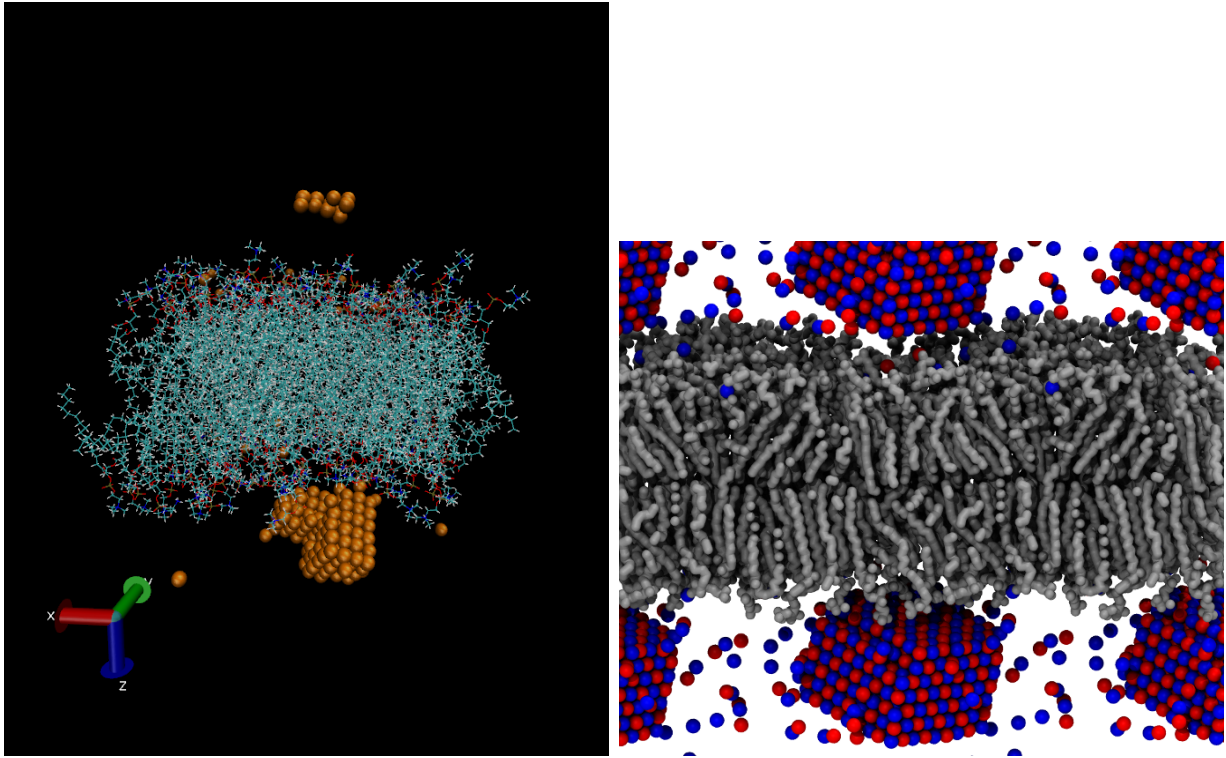


Figure S15: Ion clusters appearing in POPC:POPS (5:1) lipid17/14 simulations with 1 M of NaCl (left) and MacRog simulations with 4 M of KCl (right).

## S8 Calcium binding to POPC in CHARMM36 simulation with NBfix

The response of POPC headgroup order parameters to the CaCl<sub>2</sub> concentration are underestimated in simulations of POPC:POPS (5:1) mixture with CHARMM36 containing the NBfix for interactions between calcium and lipid oxygens<sup>72</sup> (Fig. 9 in the main text), indicating that the calcium binding to the bilayer is too weak with these parameters. Without the NBfix term, the calcium binding affinity to pure POPC lipid bilayers was overestimated in the CHARMM36 model.<sup>63</sup> However, after employing the NBfix term, the response of headgroup order parameters (Fig. S16) and the binding affinity (Fig. S17) of calcium also to a pure POPC bilayer are underestimated. Notably, CHARMM36 simulations with the NBfix terms<sup>72,73</sup> employed predict similar binding affinity for sodium and calcium. In conclusion, the special NBfix<sup>72</sup> for calcium, incorporated in the parameters give by the CHARMM-GUI at

the time of running the simulations (January 2018), leads to the underestimation of calcium binding affinity to pure PC and mixed PC:PS bilayers.

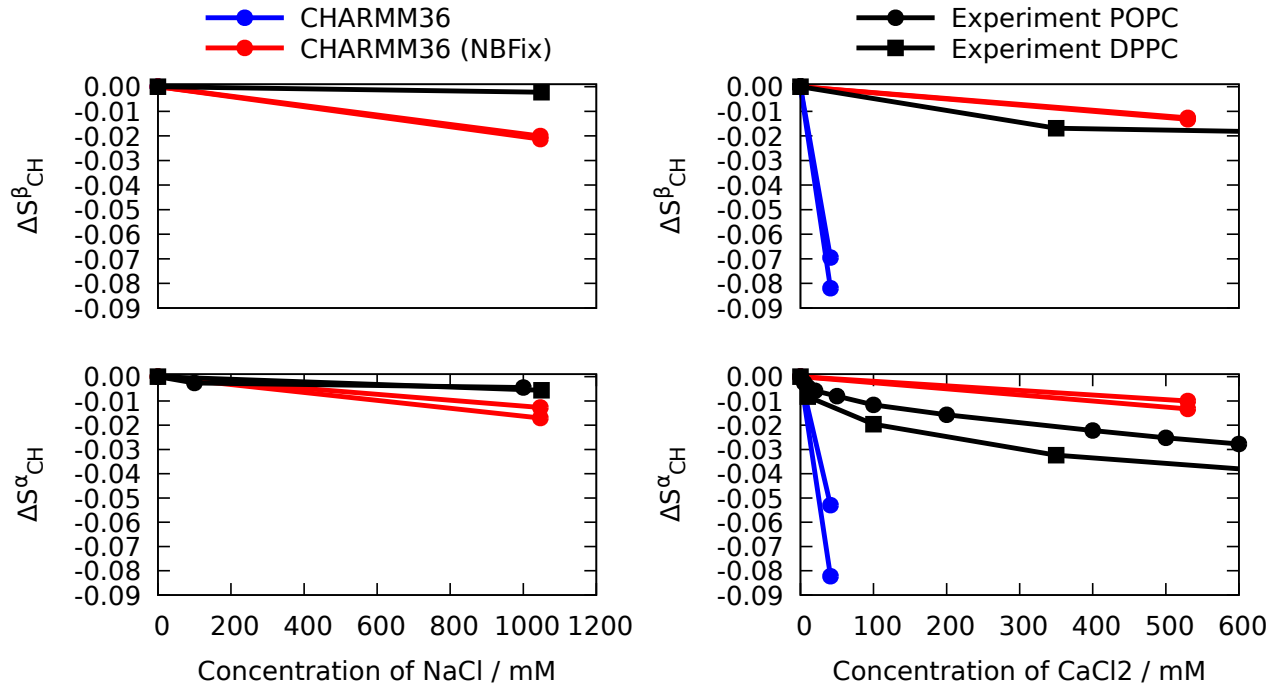


Figure S16: Headgroup order parameters from CHARMM36 simulations of POPC mixed with ions having the NBfix term employed for sodium<sup>73</sup> (*left*) and calcium<sup>72</sup> (*right*) compared with the experimental data<sup>50,51</sup> and simulations without NBfix for the calcium. Simulation files without ions are available at Ref. 74, with the NBfix term in sodium at Ref. 75, with the NBfix term in calcium at Ref. 75 and without the NBfix in calcium at Ref. 76.

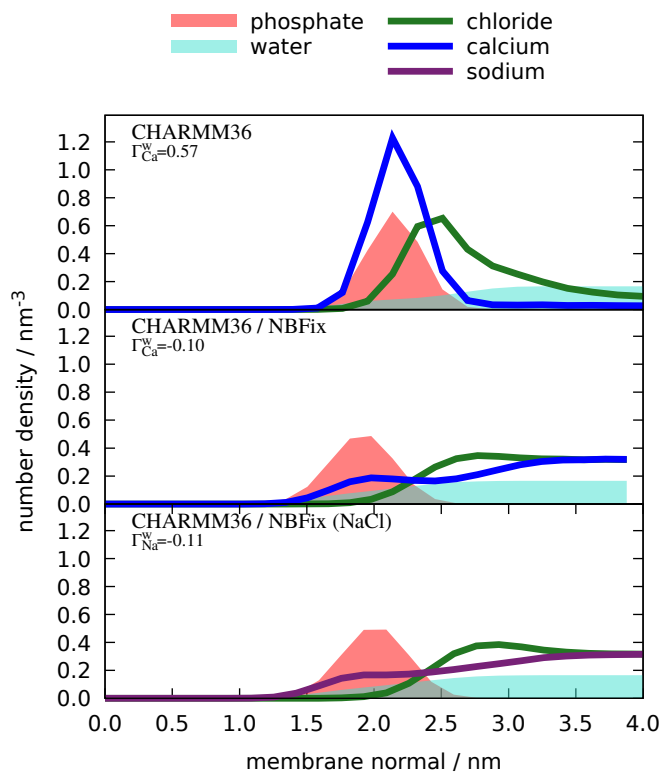


Figure S17: Density profiles along membrane normal from CHARMM36 simulations with (middle) and without (top) the NBfix term for calcium<sup>72</sup> compared to the simulation with the NBfix term for sodium<sup>73</sup> (bottom). The simulation data are the same as in figure S16.

## S9 Calcium density profiles from simulations with POPC:POPS mixture

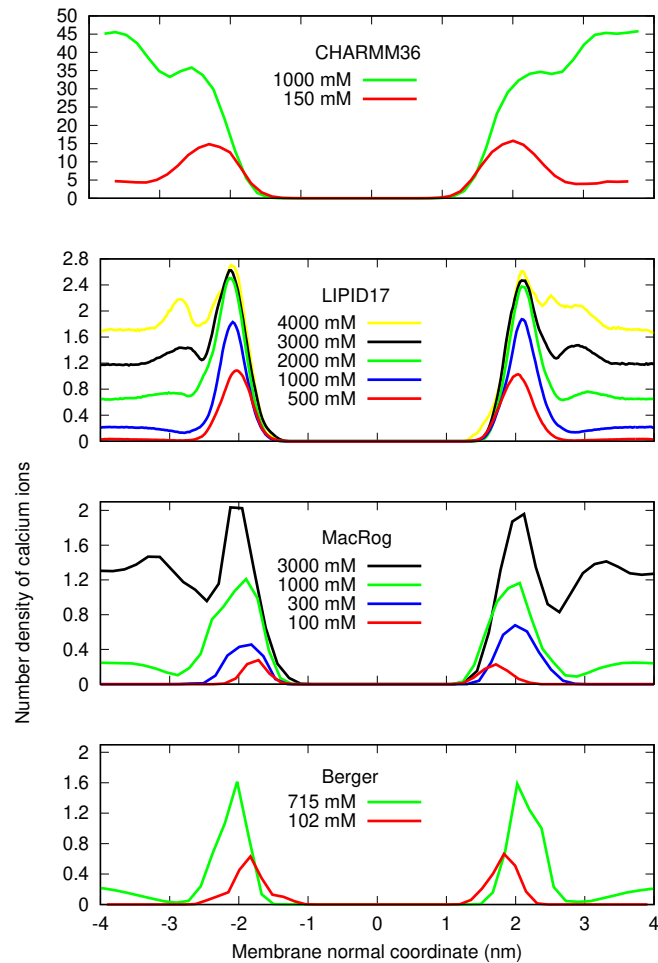


Figure S18:  $\text{Ca}^{2+}$  density profiles from simulations.

The CHARMM results are mass densities, number densities should be used when the data by Jesper Madsen is available.  
Should we include also counterions into the plot?

## S10 Details of the rough subjective force field ranking (Fig. 5)

The assessment was based fully on the Fig. 3. First, for each carbon (the columns in Fig. 3) in each force field (the rows), we looked separately at deviations in magnitude and forking.

**Magnitude** deviations, i.e., how close to the experimentally obtained C–H order parameters (OPs) the force-field-produced OPs were. For each carbon, the following 5-step scale was used:

**0 ( )**: More than half of all the calculated OPs (that is, of all different hydrogens in all different lipids) were within the *subjective sweet spots* (SSP, blue-shaded areas in Fig. 3).

**1 (M)**: All the calculated OPs were  $< 0.03$  units away from the SSP.

**2 (M)**: All the calculated OPs were  $< 0.05$  units away from the SSP.

**3 (M)**: All the calculated OPs were  $< 0.10$  units away from the SSP.

**4 (M)**: Some of the calculated OPs were  $> 0.10$  units away from the SSP.

**Forking** deviations, i.e., how well the difference in order parameters of two hydrogens attached to a given carbon matched that obtained experimentally. Note that this is not relevant for  $\beta$  and  $g_2$ , which have only one hydrogen. For the  $\alpha$  carbon, for which a considerable forking of 0.105 is experimentally seen, the following 5-step scale was used:

**0 ( )**: The distance  $D$  between the dots (that mark the measurement-time-weighted averages in Fig. 3) was  $0.08 < D < 0.13$  units for all the calculated OPs (that is, for all different lipids).

**1 (F)**:  $(0.06 < D < 0.08)$  OR  $(0.13 < D < 0.15)$ .

**2 (F)**:  $(0.04 < D < 0.06)$  OR  $(0.15 < D < 0.17)$ .

**3 (F):**  $(0.02 < D < 0.04)$  OR  $(0.17 < D < 0.19)$ .

**4 (F):**  $(D < 0.02)$  OR  $(0.19 < D)$ .

For the  $g_3$  carbon, for which no forking is indicated by experiments, the following 5-step scale was used:

**0 ( ):**  $D < 0.02$ .

**1 (f):**  $0.02 < D < 0.04$ .

**2 (F):**  $0.04 < D < 0.06$ .

**3 (F):**  $0.06 < D < 0.08$ .

**4 (F):**  $0.08 < D$ .

For the  $g_1$  carbon, for which a considerable forking of 0.13 is experimentally seen, the following 5-step scale was used:

**0 ( ):**  $0.11 < D < 0.15$ .

**1 (f):**  $(0.09 < D < 0.11)$  OR  $(0.15 < D < 0.17)$ .

**2 (F):**  $(0.07 < D < 0.09)$  OR  $(0.17 < D < 0.19)$ .

**3 (F):**  $(0.05 < D < 0.07)$  OR  $(0.19 < D < 0.21)$ .

**4 (F):**  $(D < 0.05)$  OR  $(0.21 < D)$ .

Based on these assessments of magnitude and forking deviations, each carbon was then assigned to one of the following groups: "within experimental error" (magnitude and forking deviations both on step 0 of the scales described above), "almost within experimental error" (sum of the magnitude and forking deviation steps 1 or 2), "clear deviation from experiments" (sum of magnitude and forking deviation steps from 3 to 5), and "major deviation from experiments" (sum of magnitude and forking deviation steps from 6 to 8). These groups are

indicated by colors in Fig. 4. (Note that for  $\beta$  and  $g_2$ , for which there can be no forking, the corresponding group assignment limits were: 0, 1, 2, and 3.)

Finally, the total ability of the force field to describe the headgroup and glycerol structure was estimated. To this end, the groups were given the following weights: 0 (within experimental error), 1 (almost within experimental error), 2 (clear deviation from experiments), 4 (major deviation from experiments), and the weights of the five carbons were summed up. The sum, given in the  $\Sigma$ -column of Fig. 3, was then used to (roughly and subjectively, as should be clear from the above description) rank the force fields.

## References

- (1) Botan, A.; Favela-Rosales, F.; Fuchs, P. F. J.; Javanainen, M.; Kanduč, M.; Kulig, W.; Lamberg, A.; Loison, C.; Lyubartsev, A.; Miettinen, M. S. et al. Toward Atomistic Resolution Structure of Phosphatidylcholine Headgroup and Glycerol Backbone at Different Ambient Conditions. *J. Phys. Chem. B* **2015**, *119*, 15075–15088.
- (2) Fernando, F.-R. POPC\_Glycerol\_CHARMM36\_0-10-15-20-25-35-50%CHOL. 2015; <http://dx.doi.org/10.5281/zenodo.16830>, Because of the system size, the files ONLY contain the coordinates of Glycerol saved every 10ps, this is the real contribution to the nmrlipids project.
- (3) Piggot, T. CHARMM36 DOPS simulations (versions 1 and 2) 303 K 1.0 nm LJ switching. 2017; <https://doi.org/10.5281/zenodo.1129411>.
- (4) Piggot, T. CHARMM36 POPS simulations (versions 1 and 2) 298 K 1.0 nm LJ switching. 2017; <https://doi.org/10.5281/zenodo.1129415>.
- (5) Piggot, T. CHARMM36 POPS simulations (versions 1 and 2) 298 K 1.0 nm LJ switching with K ions. 2018; <https://doi.org/10.5281/zenodo.1182654>.
- (6) Piggot, T. CHARMM36 POPS/POPC simulations (versions 1 and 2) 298 K 1.0 nm LJ switching with K ions. 2018; <https://doi.org/10.5281/zenodo.1182658>.
- (7) Piggot, T. CHARMM36 POPS/POPC simulations (versions 1 and 2) 298 K 1.0 nm LJ switching with Na ions. 2018; <https://doi.org/10.5281/zenodo.1182665>.
- (8) Lee, J.; Cheng, X.; Swails, J. M.; Yeom, M. S.; Eastman, P. K.; Lemkul, J. A.; Wei, S.; Buckner, J.; Jeong, J. C.; Qi, Y. et al. CHARMM-GUI Input Generator for NAMD, GROMACS, AMBER, OpenMM, and CHARMM/OpenMM Simulations Using the CHARMM36 Additive Force Field. *Journal of Chemical Theory and Computation* **2016**, *12*, 405–413.

- (9) Jo, S.; Kim, T.; Iyer, V. G.; Im, W. CHARMM-GUI: A web-based graphical user interface for CHARMM. *Journal of Computational Chemistry* 29, 1859–1865.
- (10) Ollila, O. H. S. POPC:POPS (5:1) with 450 mM potassium simulation with CHARMM36 at 298K. 2018; <https://doi.org/10.5281/zenodo.1493241>.
- (11) Ollila, O. H. S. POPC:POPS (5:1) with 890 mM potassium simulation with CHARMM36 at 298K. 2018; <https://doi.org/10.5281/zenodo.1493246>.
- (12) Ollila, O. H. S. POPC:POPS (5:1) with 440 mM sodium simulation with CHARMM36 at 298K. 2018; <https://doi.org/10.5281/zenodo.1493190>.
- (13) Ollila, O. H. S. POPC:POPS (5:1) with 890 mM sodium simulation with CHARMM36 at 298K. 2018; <https://doi.org/10.5281/zenodo.1493229>.
- (14) Piggot, T. CHARMM36-UA DOPS simulations (versions 1 and 2) 303 K 1.0 nm LJ switching. 2017; <https://doi.org/10.5281/zenodo.1129456>.
- (15) Piggot, T. CHARMM36-UA POPS simulations (versions 1 and 2) 298 K 1.0 nm LJ switching. 2017; <https://doi.org/10.5281/zenodo.1129458>.
- (16) Javanainen, M. Simulation of a POPC bilayer at 298K, lipid model by Maciejewski and Rog. 2018; <https://doi.org/10.5281/zenodo.1167532>.
- (17) Piggot, T. MacRog POPS simulations (versions 1 and 2) 298 K with corrected PO not OP tails. 2018; <https://doi.org/10.5281/zenodo.1283335>.
- (18) Javanainen, M. Simulation of a POPS membrane with potassium counterions. 2018; <https://doi.org/10.5281/zenodo.1434990>.
- (19) Javanainen, M. Simulations of POPC/POPS membranes with CaCl<sub>2</sub>. 2017; <https://doi.org/10.5281/zenodo.1409551>.

- (20) Javanainen, M. Simulations of POPC/POPS membranes with KCl. 2018; <https://doi.org/10.5281/zenodo.1404040>.
- (21) Miettinen, M. S.; Kav, B. Molecular dynamics simulation trajectory of an anionic lipid bilayer: 100 mol% POPS with Na<sup>+</sup> counterions using Joung-Cheetham Ions. 2018; <https://doi.org/10.5281/zenodo.1148495>, B.K. acknowledges financial support from International Max Planck Research School on Multiscale Bio-Systems.
- (22) Miettinen, M. S.; Kav, B. Molecular dynamics simulation trajectory of an anionic lipid bilayer: 100 mol% POPS with Na<sup>+</sup> counterions using ff99 ions. 2018; <https://doi.org/10.5281/zenodo.1134869>, B.K. acknowledges financial support from International Max Planck Research School on Multiscale Bio-Systems.
- (23) Kav, B.; Miettinen, M. S. Molecular dynamics simulation trajectory of an anionic lipid bilayer: 100 mol% DOPS with Na<sup>+</sup> counterions using Joung-Cheetham Ions. 2018; <https://doi.org/10.5281/zenodo.1134871>, B.K acknowledges financial support from International Max Planck Research School on Multiscale Bio-Systems.
- (24) Kav, B.; Miettinen, M. S. Molecular dynamics simulation trajectory of an anionic lipid bilayer: 100 mol% DOPS with Na<sup>+</sup> counterions using ff99 Ions. 2018; <https://doi.org/10.5281/zenodo.1135142>, B.K acknowledges financial support from International Max Planck Research School on Multiscale Bio-Systems.
- (25) Kav, B.; Miettinen, M. S. Amber Lipid17 Simulations of POPC/POPS Membranes with KCl Counterions. 2018; <https://doi.org/10.5281/zenodo.1250969>, B.K acknowledges financial support from International Max Planck Research School on Multiscale Bio-Systems.
- (26) Kav, B.; Miettinen, M. S. Amber Lipid17 Simulations of POPC/POPS Membranes with KCl. 2018; <https://doi.org/10.5281/zenodo.1227257>, B.K acknowledges financial support from International Max Planck Research School on Multiscale Bio-Systems.

- (27) Kav, B.; Miettinen, M. S. Amber Lipid17 Simulations of POPC/POPS Membranes with NaCl Counterions. 2018; <https://doi.org/10.5281/zenodo.1250975>, B.K acknowledges financial support from International Max Planck Research School on Multiscale Bio-Systems.
- (28) Kav, B.; Miettinen, M. S. Amber Lipid17 Simulations of POPC/POPS Membranes with NaCl. 2018; <https://doi.org/10.5281/zenodo.1227272>, B.K acknowledges financial support from International Max Planck Research School on Multiscale Bio-Systems.
- (29) Melcr, J. Molecular dynamics simulations of lipid bilayers containing POPC and POPS with the lipid17 force field, only counterions, and CaCl<sub>2</sub> concentrations. 2018; <https://doi.org/10.5281/zenodo.1487761>.
- (30) Ollila, S.; Hyvönen, M. T.; Vattulainen, I. Polyunsaturation in Lipid Membranes: Dynamic Properties and Lateral Pressure Profiles. *J. Phys. Chem. B* **2007**, *111*, 3139–3150.
- (31) Ollila, O. H. S. MD simulation of POPC lipids bilayer at 310K (Berger, Gromacs 3.1.4). 2018; <https://doi.org/10.5281/zenodo.1230170>.
- (32) Piggot, T. Berger POPS simulations (versions 1 and 2) 298 K 1.0 nm cut-off. 2017; <https://doi.org/10.5281/zenodo.1129425>.
- (33) Piggot, T. Berger DOPS simulations (versions 1 and 2) 303 K 1.0 nm cut-off. 2017; <https://doi.org/10.5281/zenodo.1129419>.
- (34) Jurkiewicz, P.; Cwiklik, L.; Vojtěchová, A.; Jungwirth, P.; Hof, M. Structure, dynamics, and hydration of POPC/POPS bilayers suspended in NaCl, KCl, and CsCl solutions. *Biochimica et Biophysica Acta (BBA) - Biomembranes* **2012**, *1818*, 609 – 616.

- (35) Cwiklik, L. MD simulation trajectory of a POPC/POPS (4:1) bilayer with 1M NaCl, Berger force field for lipids and ffgmx for ions. 2017; <https://doi.org/10.5281/zenodo.838219>.
- (36) Melcrová, A.; Pokorna, S.; Pullanchery, S.; Kohagen, M.; Jurkiewicz, P.; Hof, M.; Jungwirth, P.; Cremer, P. S.; Cwiklik, L. The complex nature of calcium cation interactions with phospholipid bilayers. *Sci. Reports* **2016**, *6*, 38035.
- (37) Lukasz, C. MD simulation trajectory of a POPC/POPS (4:1) bilayer with 102mM CaCl<sub>2</sub>, Berger force field for lipids, scaled charges for Ca<sup>2+</sup> and Cl<sup>-</sup>. 2017; <https://doi.org/10.5281/zenodo.887398>.
- (38) Lukasz, C. MD simulation trajectory of a POPC/POPS (4:1) bilayer with 715mM CaCl<sub>2</sub>, Berger force field for lipids, scaled charges for Ca<sup>2+</sup> and Cl<sup>-</sup>. 2017; <https://doi.org/10.5281/zenodo.887400>.
- (39) Samuli, O. O. H. POPC:POPS (4:1) simulation with Berger model at 310K. 2018; <https://doi.org/10.5281/zenodo.1475285>.
- (40) Mukhopadhyay, P.; Monticelli, L.; Tieleman, D. P. Molecular Dynamics Simulation of a Palmitoyl-Oleoyl Phosphatidylserine Bilayer with Na<sup>+</sup> Counterions and NaCl. *Biophysical Journal* **2004**, *86*, 1601 – 1609.
- (41) Piggot, T. GROMOS-CKP POPS simulations (versions 1 and 2) 298 K with Berger/Chiu NH3 charges and PME. 2017; <https://doi.org/10.5281/zenodo.1129431>.
- (42) Piggot, T. GROMOS-CKP POPS simulations (versions 1 and 2) 298 K with GROMOS NH3 charges and PME. 2017; <https://doi.org/10.5281/zenodo.1129435>.
- (43) Piggot, T. GROMOS-CKP DOPS simulations (versions 1 and 2) 303 K with Berger/Chiu NH3 charges and PME. 2017; <https://doi.org/10.5281/zenodo.1129429>.

- (44) Piggot, T. GROMOS-CKP DOPS simulations (versions 1 and 2) 303 K with GROMOS NH3 charges and PME. 2017; <https://doi.org/10.5281/zenodo.1129447>.
- (45) Piggot, T. GROMOS-CKP POPS/POPC simulations (versions 1 and 2) 298 K with GROMOS NH3 charges and PME. 2018; <https://doi.org/10.5281/zenodo.1283333>.
- (46) Piggot, T. GROMOS-CKP POPS/POPC simulations (versions 1 and 2) 298 K with Berger/Chiu NH3 charges and PME. 2018; <https://doi.org/10.5281/zenodo.1283331>.
- (47) Piggot, T. Slipids POPS simulations (versions 1 and 2) 298 K 1.0 nm cut-off with LJ-PME. 2017; <https://doi.org/10.5281/zenodo.1129441>.
- (48) Piggot, T. Slipids DOPS simulations (versions 1 and 2) 303 K 1.0 nm cut-off with LJ-PME. 2017; <https://doi.org/10.5281/zenodo.1129439>.
- (49) Favela-Rosales, F. MD simulation trajectory of a fully hydrated DOPS bilayer: SLIPIDS, Gromacs 5.0.4. 2017. 2017; <https://doi.org/10.5281/zenodo.495510>.
- (50) Akutsu, H.; Seelig, J. Interaction of metal ions with phosphatidylcholine bilayer membranes. *Biochemistry* **1981**, *20*, 7366–7373.
- (51) Altenbach, C.; Seelig, J. Calcium binding to phosphatidylcholine bilayers as studied by deuterium magnetic resonance. Evidence for the formation of a calcium complex with two phospholipid molecules. *Biochemistry* **1984**, *23*, 3913–3920.
- (52) Seelig, J.; MacDonald, P. M.; Scherer, P. G. Phospholipid head groups as sensors of electric charge in membranes. *Biochemistry* **1987**, *26*, 7535–7541.
- (53) Scherer, P. G.; Seelig, J. Electric charge effects on phospholipid headgroups. Phosphatidylcholine in mixtures with cationic and anionic amphiphiles. *Biochemistry* **1989**, *28*, 7720–7728.

- (54) Borle, F.; Seelig, J. Ca<sup>2+</sup> binding to phosphatidylglycerol bilayers as studied by differential scanning calorimetry and <sup>2</sup>H- and <sup>31</sup>P-nuclear magnetic resonance. *Chemistry and Physics of Lipids* **1985**, *36*, 263 – 283.
- (55) Macdonald, P. M.; Seelig, J. Calcium binding to mixed phosphatidylglycerol-phosphatidylcholine bilayers as studied by deuterium nuclear magnetic resonance. *Biochemistry* **1987**, *26*, 1231–1240.
- (56) Roux, M.; Bloom, M. Calcium, magnesium, lithium, sodium, and potassium distributions in the headgroup region of binary membranes of phosphatidylcholine and phosphatidylserine as seen by deuterium NMR. *Biochemistry* **1990**, *29*, 7077–7089.
- (57) Roux, M.; Neumann, J.-M. Deuterium NMR study of head-group deuterated phosphatidylserine in pure and binary phospholipid bilayers. *FEBS Letters* **1986**, *199*, 33–38.
- (58) Roux, M.; Bloom, M. Calcium binding by phosphatidylserine headgroups. Deuterium NMR study. *Biophys. J.* **1991**, *60*, 38 – 44.
- (59) Scherer, P.; Seelig, J. Structure and dynamics of the phosphatidylcholine and the phosphatidylethanolamine head group in L-M fibroblasts as studied by deuterium nuclear magnetic resonance. *EMBO J.* **1987**, *6*.
- (60) Ferreira, T. M.; Coreta-Gomes, F.; Ollila, O. H. S.; Moreno, M. J.; Vaz, W. L. C.; Topgaard, D. Cholesterol and POPC segmental order parameters in lipid membranes: solid state <sup>1</sup>H-<sup>13</sup>C NMR and MD simulation studies. *Phys. Chem. Chem. Phys.* **2013**, *15*, 1976–1989.
- (61) Ollila, O. S.; Pabst, G. Atomistic resolution structure and dynamics of lipid bilayers in simulations and experiments. *Biochimica et Biophysica Acta (BBA) - Biomembranes* **2016**, *1858*, 2512 – 2528.

- (62) Ferreira, T. M.; Sood, R.; Bärenwald, R.; Carlström, G.; Topgaard, D.; Saalwächter, K.; Kinnunen, P. K. J.; Ollila, O. H. S. Acyl Chain Disorder and Azelaoyl Orientation in Lipid Membranes Containing Oxidized Lipids. *Langmuir* **2016**, *32*, 6524–6533.
- (63) Catte, A.; Girych, M.; Javanainen, M.; Loison, C.; Melcr, J.; Miettinen, M. S.; Monticelli, L.; Maatta, J.; Oganesyan, V. S.; Ollila, O. H. S. et al. Molecular electrometer and binding of cations to phospholipid bilayers. *Phys. Chem. Chem. Phys.* **2016**, *18*, 32560–32569.
- (64) Melcr, J.; Martinez-Seara, H.; Nencini, R.; Kolafa, J.; Jungwirth, P.; Ollila, O. H. S. Accurate Binding of Sodium and Calcium to a POPC Bilayer by Effective Inclusion of Electronic Polarization. *The Journal of Physical Chemistry B* **2018**, *122*, 4546–4557.
- (65) Ollila, O. H. S. CHARMM36 simulations of POPC mixed with cationic surfactant. 2018; <https://doi.org/10.5281/zenodo.1288297>.
- (66) Melcr, J. POPC lipid membrane, 303K, Charmm36 force field, simulation files and 200 ns trajectory for Gromacs MD simulation engine v5.1.2. 2016; <https://doi.org/10.5281/zenodo.153944>.
- (67) Favela-Rosales, F. MD simulation trajectory of a lipid bilayer: Pure POPC in water. SLIPIDS, Gromacs 4.6.3. 2016. 2016; <https://doi.org/10.5281/zenodo.166034>.
- (68) Hauser, H.; Shipley, G. G. Interactions of monovalent cations with phosphatidylserine bilayer membranes. *Biochemistry* **1983**, *22*, 2171–2178.
- (69) Hauser, H.; Shipley, G. Comparative structural aspects of cation binding to phosphatidylserine bilayers. *Biochimica et Biophysica Acta (BBA) - Biomembranes* **1985**, *813*, 343 – 346.
- (70) Mattai, J.; Hauser, H.; Demel, R. A.; Shipley, G. G. Interactions of metal ions with

- phosphatidylserine bilayer membranes: effect of hydrocarbon chain unsaturation. *Biochemistry* **1989**, *28*, 2322–2330.
- (71) Cevc, G. Membrane electrostatics. *Biochim. Biophys. Acta - Rev. Biomemb.* **1990**, *1031*, 311 – 382.
- (72) Kim, S.; Patel, D.; Park, S.; Slusky, J.; Klauda, J.; Widmalm, G.; Im, W. Bilayer Properties of Lipid A from Various Gram-Negative Bacteria. *Biophysical Journal* **2016**, *111*, 1750 – 1760.
- (73) Venable, R. M.; Luo, Y.; Gawrisch, K.; Roux, B.; Pastor, R. W. Simulations of Anionic Lipid Membranes: Development of Interaction-Specific Ion Parameters and Validation Using NMR Data. *The Journal of Physical Chemistry B* **2013**, *117*, 10183–10192.
- (74) Nencini, R. Simulation data for CHARMM36 POPC bilayer, 100 lipids/leaflet, 310K, GROMACS 5.1.4. 2018; <https://doi.org/10.5281/zenodo.1198158>.
- (75) Nencini, R. Simulation data for CHARMM36 POPC bilayer, 100 lipids/leaflet, 450 mM CaCl<sub>2</sub> ("NB-Fix" used), 310K, GROMACS 5.1.4. 2018; <https://doi.org/10.5281/zenodo.1198171>.
- (76) Javanainen, M. POPC @ 310K, 450 mM of CaCl<sub>2</sub>. Charmm36 with default Charmm ions. 2016; <http://dx.doi.org/10.5281/zenodo.51185>.